Journal of Hazardous Materials 161 (2009) 307–316

Contents lists available at ScienceDirect

Journal of Hazardous Materials

journal homepage: www.elsevier.com/locate/jhazmat

The removal of reactive dyes from aqueous solutions using chemically modified mesoporous silica in the presence of anionic surfactant—The temperature dependence and a thermodynamic multivariate analysis

Antonio R. Cestari[a,*], Eunice F.S. Vieira[a], Gláucia S. Vieira[a], Luiz P. da Costa[a], Andréa M.G. Tavares[a], Watson Loh[b], Claudio Airoldi[b]

[a] Laboratory of Materials and Calorimetry, Departamento de Química/CCET, Universidade Federal de Sergipe, CEP 49100-000, São Cristóvão, Sergipe, Brazil
[b] Universidade Estadual de Campinas, Instituto de Química, CP 6154, 13083-970, Campinas, São Paulo, Brazil

ARTICLE INFO

Article history:
Received 29 January 2008
Received in revised form 19 March 2008
Accepted 20 March 2008
Available online 27 March 2008

Keywords:
Silica gel
Dye
Adsorption
Thermodynamics
Chemometrics

ABSTRACT

The three-parameter Sips adsorption model was successfully employed to modeled equilibrium adsorption data of a yellow and a red dye onto a mesoporous aminopropyl-silica, in the presence of the surfactant sodium dodecylbenzenesulfonate (DBS) from 25 to 55 °C. The results were evaluated in relation to the previously reported surface tension measurements. The presence of curvatures of the van't Hoff plots suggested the presence of non-zero heat capacities terms ($\Delta_{ads}C_p$). For the yellow dye, it is observed that the values of $\Delta_{ads}H$ are almost all positive and they decrease in endothermicity, in the absence and in the presence of DBS, from 25 to 55 °C. For the red dye, there is an increase in endothermicity in relation to the temperature increase. The negative $\Delta_{ads}G$ values indicate spontaneous adsorption processes. Almost all adsorption entropy values ($\Delta_{ads}S$) were positive. This suggests that entropy is a driving force of adsorption. The adsorption thermodynamic parameters were also evaluated using a new 2^3 full factorial design analysis. The multivariate polynomial modelings indicated that the thermodynamic parameters are also affected by important interactive effects of the experimental factors and not by the temperature changes alone.

1. Introduction

The treatment of wastewater has long been a major concern in the environmental field. The total dyes consumption of the textile industry worldwide is in excess of 10^7 kg per year, and approximately one million kilograms per year of dyes are discharged into water streams by the textile industry [1]. Unless properly treated, the dyes present in wastewaters can affect photosynthesis activity due to reduced light penetration and may also be toxic to certain forms of aquatic life [2]. The chemical structure of dyes varies enormously, and some have complicated aromatic structures that resist degradation in conventional wastewater treatment process because of their stability to sunlight, oxidizing agents and microorganism [1,2]. Methods for removing dyes from wastewaters using the adsorption technique provide effective and economical removals [1–3].

Adsorption techniques have found many practical applications for separation and purification of gaseous and liquid mixtures. Many micro–mesoporous, crystalline, and amorphous families of adsorbents, such as zeolites, activated carbons, silica and alumina gels, ion-exchange resins, and polymeric sorbents, with a wide spectrum of surface chemistry and pore structure, have been used to carry out the desired separations [4–6]. In the design of improved adsorbents for specific substances, surface modification is very helpful for the improvement of the adsorption capacity and selectivity of the adsorbents by taking advantage of specific interactions between the adsorbents and the adsorbates [7].

Silica gel is a mesoporous adsorbent of particular interest due to its stability, possible reuse, and relative rapidity in reaching equilibrium, high mechanical resistance, and high surface area. Its relative high surface area allows the binding of a large number of surface groups, and the large pore channels allow a selective adsorption of specific adsorbates [7,8]. Silica surfaces modified with specific chemical functional groups are capable of selective interactions with various chemical compounds in solution [8]. Applications of modified silicas are found, for example, in HPLC retention of polyaromatic-hydrocarbons [9], immobilization of electrochemically active Ru complexes [10] and catalytic applications for flavanone syntheses [11]. The mesoporous silica with terminal amino groups and the aminopropyl-silica synthesized by using the emulsion

* Corresponding author. Tel.: +55 792 1056656; fax: +55 792 1056651.
E-mail address: cestari@ufs.br (A.R. Cestari).

0304-3894/$ – see front matter © 2008 Elsevier B.V. All rights reserved.
doi:10.1016/j.jhazmat.2008.03.091

route technique have also been used as coupling agent in pigment or organic dye systems [12,13–15].

When a surfactant is present in aqueous solution, attractive forces between dye/surfactant result in the formation of micellar species of different sizes and stabilities. The micellar species create a counterbalancing mechanism against dye-fibre attractive forces, and control the adsorption of the dye on the fibre [1–4]. So, the strength and stability of dye–surfactant interactions are of great importance for dyeing processes [16].

After the dyeing process, surfactants are released into wastewaters in high amounts. The adsorption of dyes onto solid sorbents is influenced dramatically by the presence of surfactants. However, almost nothing is known about the adsorption behavior of dyes at the solid/solution interface in the presence of surfactants.

In this work, a three-parameter equilibrium adsorption model – the Sips model – was used to evaluate the interactions of two selected anionic dyes with a mesoporous aminopropylsilane-silica in aqueous medium. The influence of temperature and the presence of the anionic surfactant sodium dodecylbenzenesulfonate (DBS) on the adsorption thermodynamic parameters, using a 2^3 full multivariate analysis were also presented and discussed.

2. Materials and methods

2.1. Materials

Silica gel 60 (Merck), for column chromatography, presenting particle size and average pore size of 60–230 mesh and 60 Å, respectively, was used in the present work. Before use, it was heated at 150 °C for 12 h on a vacuum line. All chemicals used were reagent grade. The silylating agent 3-(trimethoxysilyl)propylamine, 99% pure (hereafter called APTS for simplicity), from Aldrich, and sodium dodecylbenzenesulfonate, 97% pure (hereafter called DBS for simplicity), from Sigma, were used without purification.

The dyes, commercially available as Reactive Yellow GR (hereafter called yellow dye) and Reactive Red RB (hereafter called red dye) were gifts from Santista Textile Industries (Sergipe/Brazil), and were from the Dystar Dyes Company. Fig. 1 shows the chemical structures of the dyes. The purity of both dyes is 55%, due to the presence of inert materials in the commercial samples of the dyes.

2.2. Synthesis and characterization of the aminated-silica

The synthesis of the aminopropyl-silica followed the procedure described elsewhere [17]. Briefly, about 50 g of activated silica was immersed in 200 mL of dry xylene and 20 mL of APTS was added. The suspension was mechanically stirred under solvent reflux for 48 h. The resulting alkoxysilane-modified silica gel (hereafter called as Sil-NH_2 for simplicity), was filtered, washed with xylene, ethanol and ethylic ether, and conditioned in a dark air-free flask, in order to prevent interactions between the immobilized amino groups and atmospheric CO_2 [18].

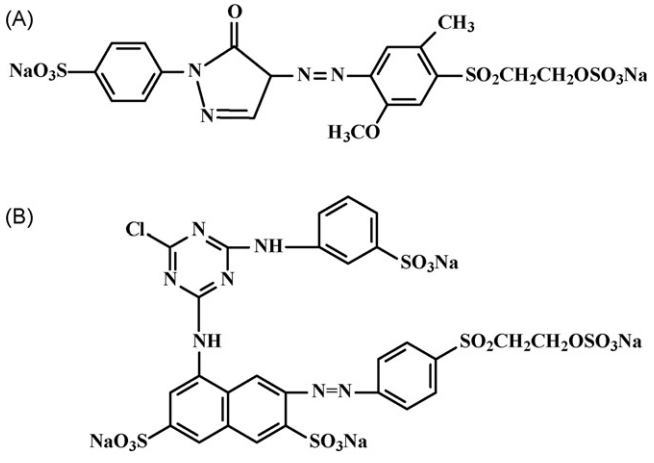

Fig. 1. Chemical structures of the reactive dyes yellow dye (A, above), and red dye (B, below).

The thermogravimetric analyses (TG) were made using about 10 mg of the unmodified silica and Sil-NH_2, in separated runs, under synthetic-air atmosphere at 10 °C min^{-1}, from 25 to 1000 °C, in a SDT 2960 thermoanalyzer, from TA Instruments.

The amount of nitrogen of the Sil-NH_2 was made by the Kjeldhal method and checked by TG [16]. The surface areas of the silicas were determined in a FlowSorb 2300 surface area analyser from Micromeritics Instruments, using the BET N_2 adsorption methodology [19,20].

2.3. Equilibrium adsorption of anionic dyes on the aminopropyl-silica

Acetic acid/sodium acetate buffered solutions at pH 4.0 were used as solvent, because the adsorption of anionic dyes is maximized at this pH value [21]. In addition, the silica-attached aminopropyl molecule can be affected, even removed from the silica surface, when very acidic solutions (pH less than 3.5) are used [21]. The adsorption experiments were performed by batch procedures, from 25 to 55 ± 0.1 °C, using dyes aqueous solutions from 20.0 to 800 mg L^{-1}. In each adsorption experiment, 50 mL of the dye solution was added to 100 mg of the Sil-NH_2 in a 150 mL polyethylene flask, and stirred continuously at a determined temperature. The shaking time of 200 min was established earlier as sufficient for the establishment of all adsorption equilibria [17]. At equilibrium times samples were taken and the dye concentration was determined spectrophotometrically at 430 and 530 nm, for the yellow and red dye, respectively.

In order to evaluate the role of the DBS surfactant, the adsorption experiments were also carried-out with the presence of the DBS surfactant, using the proportions dye/DBS of 1:1, in mg L^{-1}. This proportion was chosen in order to check possible adsorption competitions of the dyes and the DBS for the adsorption sites of the Sil-NH_2. The maximum absorbances of the dyes solutions were checked for each solution with a specific DBS concentration.

The adsorbed dye quantities were calculated using the expression [17]:

$$Q_e = \frac{(C_i - C_{eq})V}{m} \quad (1)$$

where Q_e is the fixed quantity of dye per gram of Sil-NH_2 at equilibrium in mg g^{-1}, C_i is the initial concentration of dye in mg L^{-1}, C_{eq} is the concentration of dye present at equilibrium in mg L^{-1}, V is the volume of the solution in L and m is the mass of Sil-NH_2 in g.

The equilibrium non-linear modeling of the adsorption data, as well as the multivariate calculations (*t*-tests, *F*-tests, analysis of variance (ANOVA), multiple regressions and Pareto charts) was performed using the software packages ORIGIN® and Statistica®, both release 7.0.

3. Results and discussion

3.1. Preliminary considerations

The dyes and DBS micellar species interactions on the Sil-NH_2 surface are principally electrostatic in nature [22].

The TG curves of the unmodified and Sil-NH_2 silicas are shown in Fig. 2. The first mass losses steps, from about 25 to 120 °C, are

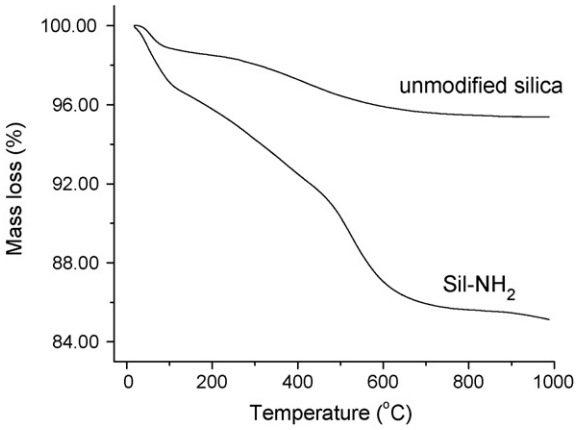

Fig. 2. TG curves of unmodified and Sil-NH_2 silicas.

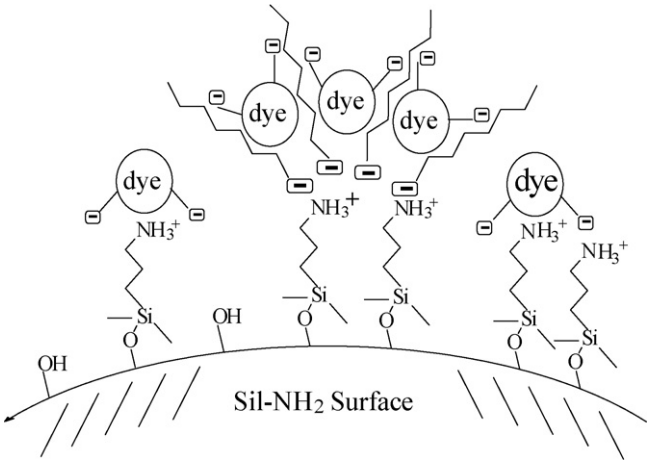

Fig. 3. Schematic representation of the interactions of the dyes with the Sil-NH_2 silica in the presence of an anionic surfactant.

due to the loss of physically adsorbed water on the surfaces [23]. The second mass losses steps, from 120 to about 980 °C, are due to the loss of immobilized aminopropyl groups for the Sil-NH_2. The quantities of mass losses (second stages) are 3.35% and 11.67%, for the unmodified and Sil-NH_2 silicas, respectively. However, since the silica silanization reaction use about 50% of the total content of the silanol groups of the silica [18], the second mass loss stage for Sil-NH_2 is also attributed to the loss of water from the condensation of the residual unreacted silanol groups [18]. From the TG quantitative analysis methodology [18] of the second stage mass loss a quantity of 5.00% (28.5 mg of N g^{-1} of Sil-NH_2) of amine groups (error analysis of ±0.15%) was found. The Kjeldhal analysis of the Sil-NH_2 showed the presence of 30.0 mg of N g^{-1} of Sil-NH_2.

The Kjeldhal analysis of the Sil-NH_2 showed the presence of 30.0 mg of N g^{-1} of Sil-NH_2. The surface area analyses were 300 and 190 m^2 g^{-1} of material, for the unmodified silica and Sil-NH_2, respectively. The decrease of the surface areas reflects the occupation of small pores of the silica by the APTS molecules [18,19].

Surfactants are used very often to modify the surface properties of various materials, such as their surface charge or hydrophobicity/hydrophilicity. In this way, the sorption of various substances (typically organic compounds) can be supported (coadsorption), or even the sorption of normally non-retained species may be enabled (adsolubilization) [16,22]. However, a prediction of the effects of surfactants on sorption is not easy, as several simultaneous and competitive mechanisms may be operating during the sorption process. In general, at low DBS concentrations, the dye sorption increased with increasing surfactant concentration. At high DBS concentrations, on the other hand, the dye sorption was suppressed steeply as a result of the complete micelle formation and dye solubilization [16,22]. The schema of Fig. 3 represents a general view of the possible interactions that occur with the Sil-NH_2 and the dyes in the presence of DBS. The interactions of the dyes with the Sil-NH_2 are represented by the "free dyes" in solution and by the dyes/DBS aggregates, according to references [17].

The critical aggregation concentration (cac) values for each dye/DBS system were presented and discussed earlier [17]. Briefly, it is observed that the cac values of the yellow dye increase from 25 to 45 °C (from 41.37 to 50.32 mg L^{-1}) and decrease from 45 to 55 °C (from 50.32 to 38.72 mg L^{-1}). This behavior has been related to difficulties of the dye/surfactant interactions at low temperatures due to the relative high hydrophilic/hydrophobic ratio for planar molecules, such as the yellow dye. So, the dye/surfactant hydrophobic interactions do not occur at higher magnitudes. At high temperatures, the relative dehydration of the hydrophobic parts of the yellow dye carbonic chains enables easier yellow dye/DBS interactions [17]. On the other hand, the cac results for the red dye/DBS aggregates decrease (from 124.52 to 88.50 mg L^{-1}) with the temperature increasing. The higher cac results, in relation to the yellow dye, seem to be related to the more ramified chemical structure of the red dye, which do not allow the formation of the dye/DBS hydrophobic interactions cited above in a high extension.

The cac of the DBS was 95.50 mg L^{-1}. This value did not show alterations in relation to the temperature increasing. The differences of the cac values of the dyes-DBS aggregates have been related to the different interactions of the hydrophobic microdomains of the dyes with the surfactant micelles [17]. In the present study, the hydrophobic interactions of the aggregates yellow dye/DBS seem to be higher than the red dye/DBS due to, probably, the relative small chemical structure of the yellow dye [17]. The lower affinity suggested for the red dye/DBS aggregates may also due to negative charge–charge repulsions of the sulfonate groups of the red dye chemical structure. On the other hand, the differences of the cac values may also be due to a combination of interactions in the hydrophobic region of the mixed micelles and the polar micelle–water interface [17].

3.2. Adsorption of the anionic dyes on Sil-NH_2

We have used the yellow and the red dye because their chemical structures present significant differences to each other. The yellow dye presents a planar structure and the red dye presents a more ramified chemical structure. This criterion has been used in our adsorption studies. The results have been shown that the differences cited in the chemical structures of the dyes have been provided significant differences in the amounts adsorbed, as well as in the kinetic and thermodynamic parameters [17,18].

The adsorption data were tentatively adjusted to the three-parameter Sips adsorption model, shown in Eq. (2). In this model, it incorporates the features of the classical Langmuir and Freundlich adsorption models [24]:

$$Q_e = \frac{q^m b(C_{eq})^{1/n_S}}{1 + b(C_{eq})^{1/n_S}} \quad (2)$$

where C_{eq} is the final concentration (mg/L) in the supernatant at equilibrium for each initial concentration, q^m is the maximum adsorption capacity at a given temperature, b is a constant related to the energy of the adsorption, and $1/n_S$ is the Sips parameter related to the intensity of the adsorption. The Sips isotherm contains three parameters adjustable (q^m, b and $1/n_S$) and these were found from non-linear procedures. The Sips adsorption parameters are presented in Table 1.

Table 1
The Sips adsorption parameters of the interaction for the yellow and red dyes in the absence and in the presence of the anionic surfactant DBS

Dye	T (°C)	In the absence of DBS			In the presence of DBS		
		q^m (mg g^{-1})	$b/10^{-3}$(L mg^{-1})$^{1/n_S}$	$1/n_S$	q^m (mg g^{-1})	$b/10^{-3}$(L mg^{-1})$^{1/n_S}$	$1/n_S$
Yellow	25	21.1	9.60	2.25	92.9	7.20	1.11
	35	22.8	108	1.15	81.6	1.60	1.95
	45	26.9	93.0	1.00	69.6	0.60	2.58
	55	30.5	100	1.06	64.3	0.98	2.57
Red	25	11.1	0.23	2.02	37.8	51.0	3.00
	35	14.0	9.70	1.14	54.5	39.0	2.70
	45	11.8	100	1.00	62.4	79.0	1.90
	55	11.9	155	1.00	60.8	192	1.98

In order to quantitatively compare the applicability of the Sips model, Table 1 shows normalized standard deviations (ΔQ_e), which are obtained as follows [17]:

$$\Delta Q_e(\%) = \frac{100}{N}\sum\left|\frac{Q_{e,exp} - Q_{e,calc}}{Q_{e,exp}}\right| \quad (3)$$

where $Q_{e,calc}$ are the calculated adsorption values from the Sips adsorption model and N is the number of experimental points on a given adsorption curve.

It is observed that the Sips isotherms have good fits (in general, $\Delta Q_e \leq 10\%$) for the interactions of both dyes in the absence and in the presence of DBS at various temperatures.

The adsorption plots are shown in Figs. 4 and 5. In the absence of DBS, it is observed that the adsorption of both dyes increases with the increase in temperature from 25 to 55 °C. However, the quantitative adsorption plot profiles present different aspects in relation to the type of dye. For the yellow dye adsorption, its relatively smaller and planar chemical structure seems to contribute to its diffusion into the large-size pores of Sil-NH_2. On the other hand, the quantitative interaction of the red dye is lower than that of yellow dye. So, the adsorption of the red dye, which presents both a relatively larger size and asymmetric chemical structure, occurs, in general, with the adsorption sites on the surface of the Sil-NH_2. The role of the presence of DBS in solution in the quantitative adsorption of the dyes was discussed previously [17].

Adsorption at the solid/solution interface is expected to take place both on the external and on the internal surface. In case of adsorption at the external surface, the adsorption rate is controlled by the diffusion of the surfactant species from the bulk solution towards the external surface of the solid. The adsorption of surfactant species (monomers and/or micelles) into the internal adsorbent surface is also controlled by internal diffusional processes.

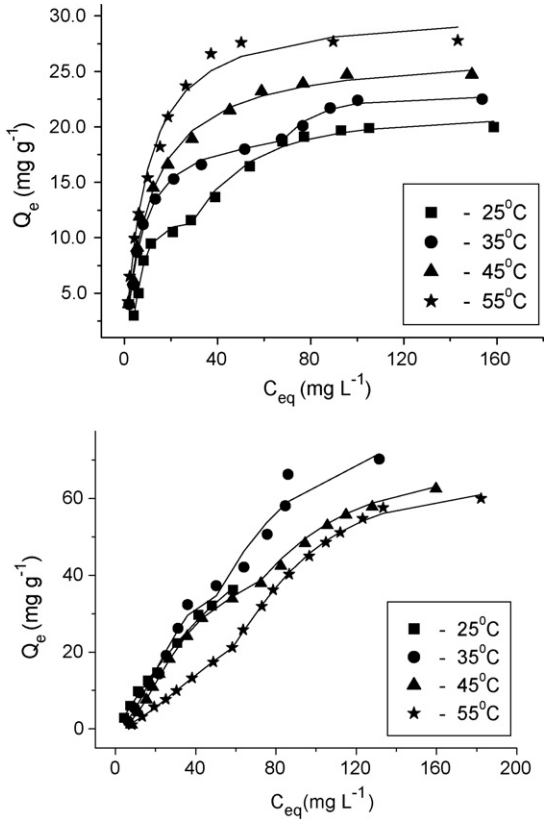

Fig. 4. Adsorption profile of the yellow dye in the absence (upper part) and in the presence (lower part) of the surfactant DBS at different temperatures. Experimental data are reported as points and the calculated data from the Sips model parameters as curves.

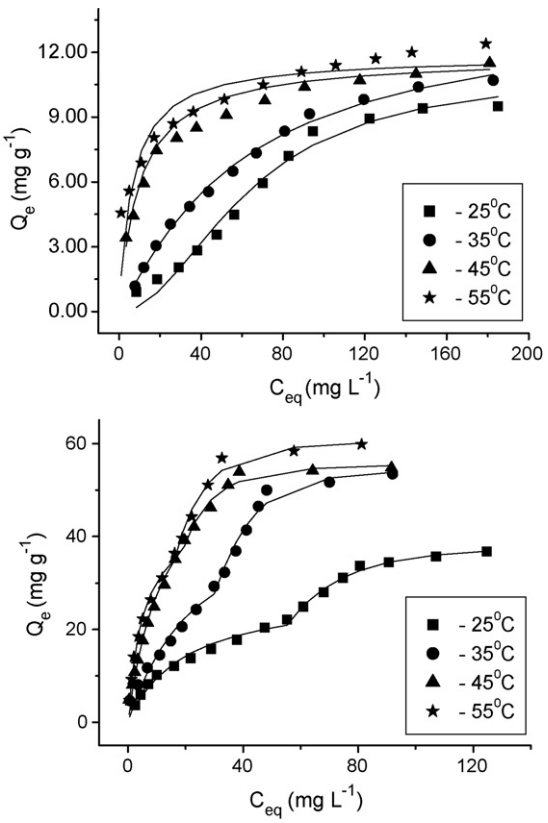

Fig. 5. Adsorption profile of the red dye in the absence (upper part) and in the presence (lower part) of the surfactant DBS at different temperatures. Experimental data are reported as points and the calculated data from the Sips model parameters as curves.

Those latter diffusion processes depend on the pore size of the adsorbent through which the surfactant molecules (in the complete micelle form, above both the cmc of the surfactant and the cac of the dye-surfactant aggregates) move to the internal adsorption sites.

In the presence of DBS, the adsorption values for the yellow dye decrease and for the red dye increase within the temperature range from 25 to 55 °C. These results reflect the differences of the dye–DBS aggregates. As shown earlier from the cac values of the dye–DBS aggregates, the interaction yellow dye–DBS is greater than the interaction red dye–DBS. So, the yellow dye–DBS micellar structures seem to adsorb, in general, using the adsorption sites of the Sil-NH_2 surface. Thus, a temperature increase reduces the adsorption values for the yellow dye, due to the weakness of the electrostatic interactions as the temperature increases. The temperature adsorption profiles of the red dye in the presence of DBS are similar to those in absence of the surfactant. However, the additional solubilization of this dye in the presence of DBS also seems to contribute to increase its adsorption amounts as the adsorption temperature increases.

3.3. Thermodynamics of adsorption of the reactive dyes on Sil-NH_2

The equilibrium constants (K) were calculated as recommended by Limousin et al. [21] using Eq. (7), in relation to the general chemical equilibrium as follows [21]:

$$\text{Sil-NH}_{2(s)} + \text{dye(eq)}_{(aq)} \rightleftharpoons \text{Sil-NH}_2/\text{dye}_{(s)}$$

$$K = \frac{(\text{Sil-NH}_2/\text{dye})}{(\text{Sil-NH}_2)(\text{dye})} \quad (4)$$

$$K = \frac{\theta}{(1-\theta)}\frac{1}{C_{eq}} \quad (5)$$

where θ is the fraction of adsorption sites that are occupied by adsorbate (free dye and/or dye/DBS aggregates), and $(1-\theta)$ is the fraction of unoccupied adsorption sites. C_{eq} is the equilibrium concentration (mol L^{-1}) of dye in solution.

For a given isotherm, the fraction of adsorption sites is defined as $\theta = Q_e/Q_e^{max}$, where Q_e^{max} is the maximum adsorption capacity. Thus, the equilibrium constants can now be expressed as:

$$K = \frac{Q_e/Q_e^{max}}{1-(Q_e/Q_e^{max})}\frac{1}{C_{eq}} \quad (6)$$

or equivalently:

$$K = \frac{Q_e}{Q_e^{max}-Q_e}\frac{1}{C_{eq}} \quad (7)$$

The values of K were found as average values of the first ten points of each isotherm, due to the high dispersion of K values (S.D. more than 20%) when the last four points of the isotherms were used. In the presence of DBS, the average K values were calculated after the cac values for each dye/DBS aggregates, where the presence of DBS monomers is supposed to be negligible [16,17,22].

The thermodynamic parameters, namely the enthalpy of adsorption ($\Delta_{ads}H$), the Gibbs free energy of adsorption ($\Delta_{ads}G$) and the entropy of adsorption ($\Delta_{ads}S$) were calculated as shown in Eqs. (8)–(10) [17]

$$\frac{\partial(\ln K)}{\partial(1/T)} = -\frac{\Delta_{ads}H}{R} \quad (8)$$

$$\Delta_{ads}G = -RT\ln K \quad (9)$$

$$\Delta_{ads}G = \Delta_{ads}H - T\Delta_{ads}S \quad (10)$$

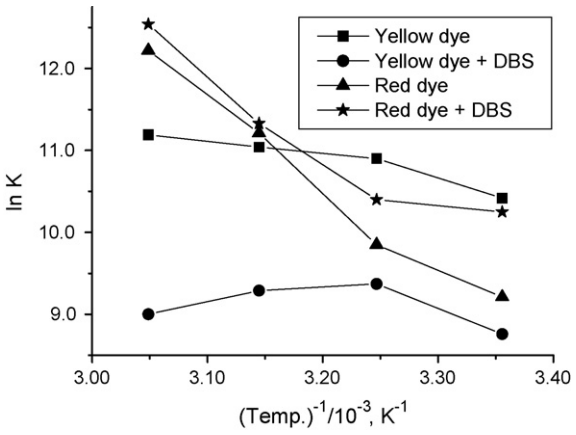

Fig. 6. The van't Hoff plots of the interactions of the dyes with Sil-NH_2 in the absence and in the presence of the surfactant DBS.

T is the solution temperature (Kelvin) and R is the gas constant (8.314 J K^{-1} mol^{-1}).

The enthalpies of the dye-Sil-NH_2 adsorption ($\Delta_{ads}H$) are found from the van't Hoff plots: $\ln K \times 1/T$ (Fig. 6). The use of the van't Hoff plots is an indirect, but accurate methodology to calculate thermodynamical adsorption parameters at solid/solution interfaces, as showed earlier using comparative data from direct isothermal titration calorimetry [25,26]. In general, adsorption enthalpies are assumed to be invariable in relation to temperature. However, difficulties arise from this assumption, which is often not the case [23]. Taking into account the curvatures of the van't Hoff plots suggested in Fig. 6, a second-order polynomial regression analysis of the van't Hoff plots was used. The general equation of this type of analysis is: $\ln K = A + B(1/T) + C(1/T)^2$, where A, B and C are the regression coefficients. The $-(\Delta_{ads}H/R)$ values were found from derivation of each individual regression functions. It was found that the polynomial regression produced better fits (r^2 values from 0.990 to 0.999) in relation to the traditional van't Hoff plots linear regressions (less than 0.900). Thus, the curvatures indicate temperature dependences of $\Delta_{ads}H$, characterized by non-zero $\Delta_{ads}C_p$ terms, used to describe the change in heat capacity. The $\Delta_{ads}C_p$ values were calculated, in a simplified manner, as follows [26]:

$$\Delta_{ads}C_p = \frac{\Delta_{ads}H_{T_2} - \Delta_{ads}H_{T_1}}{(T_2 - T_1)} (\text{where } T_2 > T_1) \quad (11)$$

The thermodynamic parameters are shown in Table 2. The variation of the thermodynamic parameters with the adsorption temperatures is shown in Figs. 7–9. For the yellow dye, it is observed that the values of $\Delta_{ads}H$ are almost all positive and they decrease in endothermicity, in the absence and in the presence of DBS, at the temperatures 25 and 55 °C. For the red dye, the opposite situation for $\Delta_{ads}H$ behavior is observed, i.e., there is an increase in endothermicity in relation to the temperature increase. One possible explanation of the general tendency for the $\Delta_{ads}H$ values is the well-known fact that dyes and silicate surfaces are both well solvated in water. In order for the dyes to be adsorbed, they have to lose part of their hydration shell. The dehydration processes of the dyes and the adsorbent surface require energy. So, in general, the dehydration processes supersede the exothermicity of the adsorption processes. In summary, we may say that the removal of water from the dyes and the Sil-NH_2 surface is essentially an endothermic process and it appears that endothermicity of the desolvation processes, in most cases in this study, exceeds that of the exothermicity provided by the heat of adsorption. The values and analysis of the previously reported adsorption energy parameter (E), from the Dubinin–Radushkevick equation, seem to confirm the general ion-

Table 2
Thermodynamic parameters for the interaction of the yellow and red dyes in the absence and in the presence of the anionic surfactant DBS

Dye	T (°C)	In the absence of DBS					In the presence of DBS				
		ln K	$\Delta_{ads}H$ (kJ mol^{-1})	$-\Delta_{ads}G$ (kJ mol^{-1})	$\Delta_{ads}S$ (J K^{-1} mol^{-1})	$\Delta_{ads}C_p$ (kJ K^{-1} mol^{-1})	ln K	$\Delta_{ads}H$ (kJ mol^{-1})	$-\Delta_{ads}G$ (kJ mol^{-1})	$\Delta_{ads}S$ (J K^{-1} mol^{-1})	$\Delta_{ads}C_p$ (kJ K^{-1} mol^{-1})
Yellow	25	10.40	38.18	25.8	215	−1.22	8.76	60.47	21.7	276	−3.67
	35	10.86	25.15	27.9	172		9.37	21.35	23.9	147	
	45	11.08	12.93	29.2	132		9.29	−17.76	24.6	21	
	55	11.16	1.46	30.5	98		9.00	−49.77	24.5	−77	
Red	25	9.21	52.72	22.8	253	2.11	10.25	−7.77	25.4	59	4.21
	35	9.85	75.18	25.2	325		10.40	42.57	26.6	224	
	45	11.21	96.22	29.6	396		11.33	89.74	29.9	376	
	55	12.22	116.0	33.3	455		12.54	134.0	34.2	513	

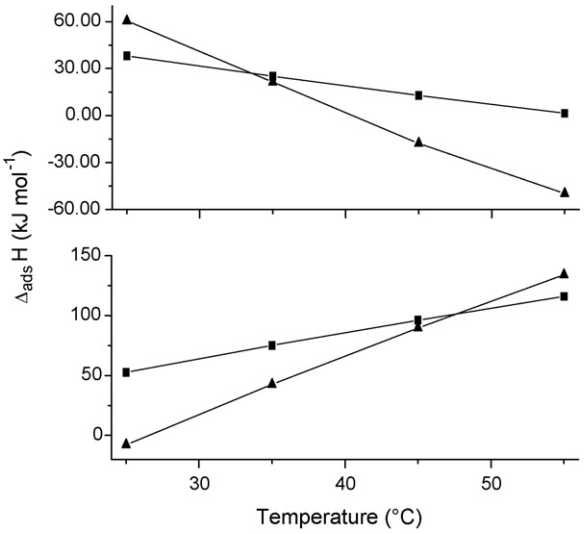

Fig. 7. Profiles of adsorption enthalpies ($\Delta_{ads}H$) of the yellow (upper figure) and the red dye (lower figure) in the absence (squares) and in the presence (triangles) of the surfactant DBS.

exchange character of the adsorption processes of this work [17]. However, we are unable to point out the extension of those desolvation processes, as well as the degree of solvation of each dye used in this work. We think that additional computational calculations should be used in future, in order to obtain more specific information concerning the adsorption thermodynamic data in relation to the type of dye and temperature. Difficulties also arise from the understanding of the correct fraction of solvent released from both the dyes molecules in solution and the Sil-NH_2 surface at a given temperature. The unreacted silanol groups present on Sil-NH_2 surface can also contribute to adsorption and release of the water present on these silanols to the solution. The endothermic enthalpy of dehydration of silica can reach values of about 30–100 kJ mol^{-1} [27].

From the inspection of Table 2, the signs of the $\Delta_{ads}C_p$ values are negative for the yellow dye, in the absence and in the presence of DBS. However, positive values are found for the red dye. In general, negative (often large) values of $\Delta_{ads}C_p$, coupled with

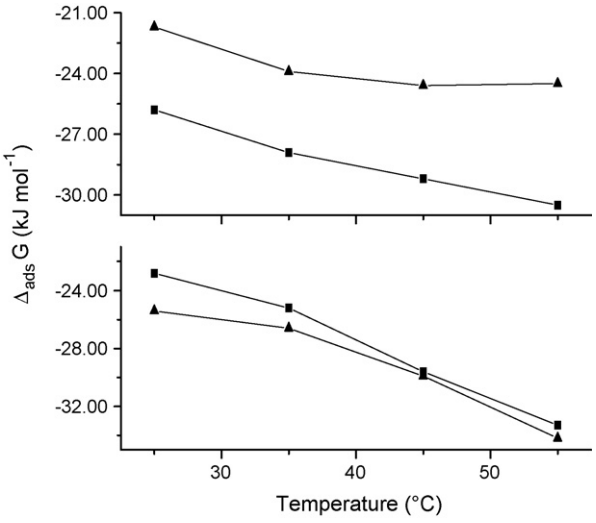

Fig. 8. Profiles of adsorption Gibbs free energies ($\Delta_{ads}G$) of the yellow (upper figure) and the red dye (lower figure) in the absence (squares) and in the presence (triangles) of the surfactant DBS.

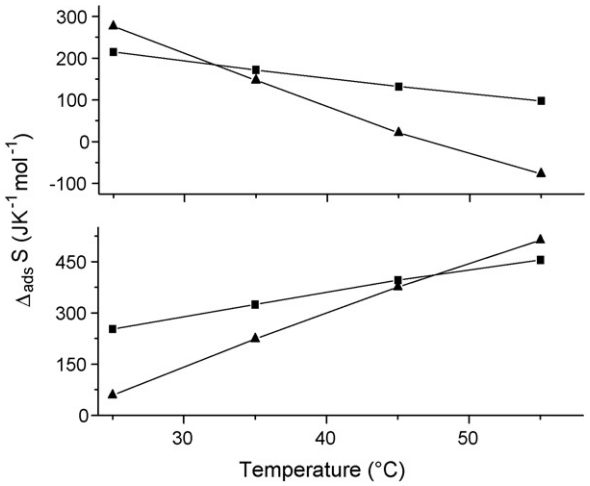

Fig. 9. Profiles of adsorption entropies ($\Delta_{ads}S$) of the yellow (upper figure) and the red dye (lower figure) in the absence (squares) and in the presence (triangles) of the surfactant DBS.

Table 3
Factors and levels used in the 2^3 factorial design study

Factors	Levels	
	(−)	(+)
(D) = Dye type	Yellow	Red
(S) = Presence of surfactant DBS[a]	No	Yes
(T) = Temperature, (°C)	25	55

[a] The proportion of DBS/dye was 1:1 in relation to the dye concentration in solution.

favorable positive entropy changes, have been used as an indicator of intense hydrophobic interactions [26]. On the other hand, positive $\Delta_{ads}C_p$ values, as observed for the red dye, in the absence and in the presence of DBS, are often related to the presence of thermal dehydration-stable species in solution, as observed in thermophilic and hyperthermophilic proteins [26].

The $\Delta_{ads}G$ values are all negative and very similar to one another. In general, binding of an adsorbate in solution is favored if $\Delta_{ads}G$ is negative. This general tendency was not changed by the presence of DBS and the temperature increase.

The positive adsorption entropy values for almost all values for the interaction of the dyes, in the absence and in the presence of DBS, indicate an increase of disorder. The $\Delta_{ads}S$ values are almost all positive for adsorption of dyes in the absence and in the presence of DBS. Thus, from the thermodynamic viewpoint, entropy seems to be a driving force of adsorption [28]. The entropic factor becomes relatively more important than enthalpy when adsorption is evaluated at high coverages of the solid adsorbent. This fact may be related to the extent of hydration of the dye molecules. The reorientation or restructuring of water around the dyes is very unfavorable in terms of entropy, because it disturbs the existing water structure and imposes a new and more ordered structure at the solid–solution interface during dye adsorption [26–28].

Table 5
Effect values for the thermodynamic parameters of the interactions of the anionic dyes with Sil-NH_2

Effects	$\Delta_{ads}H$ (kJ mol^{-1})	$\Delta_{ads}G$ (kJ mol^{-1})	$\Delta_{ads}S$ (J K^{-1} mol^{-1})
Average	43.16 ± 1.28	−27.25 ± 0.50	224 ± 5
Principal			
D	61.16 ± 2.56	−3.25 ± 1.00	193 ± 10
S	−17.85 ± 2.56	1.70 ± 1.00	−63 ± 10
T	14.53 ± 2.56	−6.75 ± 1.00	46 ± 10
Interactions			
D–S	−3.39 ± 2.56	−3.35 ± 1.00	−7 ± 10
D–T	87.99 ± 2.56	−3.00 ± 1.00	280 ± 10
S–T	1.23 ± 2.56	−0.10 ± 1.00	5 ± 10
D–S–T	38.01 ± 2.56	0.85 ± 1.00	123 ± 10

3.3.1. Evaluation of adsorption thermodynamics by multivariate analysis

A full 2^3 factorial design was performed to evaluate the importance of the type of dye, the presence of the surfactant DBS and temperature. Table 3 summarizes these factors and their respective levels.

Principal and interaction effect values are easily calculated from factorial design results. Both types of effects are calculated using the Eq. (2) [29].

$$\text{Effect} = \bar{R}_{+,i} - \bar{R}_{-,i} \quad (12)$$

where $\bar{R}_{+,i}$ and $\bar{R}_{-,i}$ are the average values of Q_e for the high (+) and low (−) levels of each factor. For principal or main effects the above averages simply refer to the results at the high (+) and low (−) levels of the factor whose effect is being calculated independent of the levels of the other factors. For binary interactions $\bar{R}_+$ is the average of results for both factors at their high and low levels whereas $\bar{R}_-$ is the average of the results for which one of the factors involved is at the high level and the other is at the low level. In general, high-order interactions are calculated using the above equation by applying signs obtained by multiplying those for the factors involved, (+) for high and (−) for low levels. If duplicate runs are performed for each individual measurement, as done in this work, standard errors (E) in the effect values can be calculated by [29]:

$$E = \{\Sigma(d_i)^2/8N\}^{1/2} \quad (13)$$

where d_i is the difference between each duplicate value and N is the number of distinct experiments performed.

The results obtained in a factorial design depend, in part, on the ranges of the factors studied. The chosen levels should be large enough to provoke response changes that are larger than experimental error. However, these differences should not be so large that quadratic or higher order effects due to the individual factors become important and invalidate the factorial model. Under these conditions factorial designs are particularly efficient for evaluating

Table 4
Results of the adsorption thermodynamics of the 2^3 factorial design for the interactions of the anionic dyes with the Sil-NH_2

Experiment	D	S	T	$\Delta_{ads}H$ (kJ mol^{-1})	$-\Delta_{ads}G$ (kJ mol^{-1})	$\Delta_{ads}S$ (J K^{-1} mol^{-1})
1	−1	−1	−1	38.15	25.8	215
2	1	−1	−1	52.72	22.8	253
3	−1	1	−1	60.47	21.7	276
4	1	1	−1	−7.77	25.4	59
5	−1	−1	1	1.46	30.5	98
6	1	−1	1	116.00	33.3	455
7	−1	1	1	−49.77	24.5	−77
8	1	1	1	134.00	34.2	513

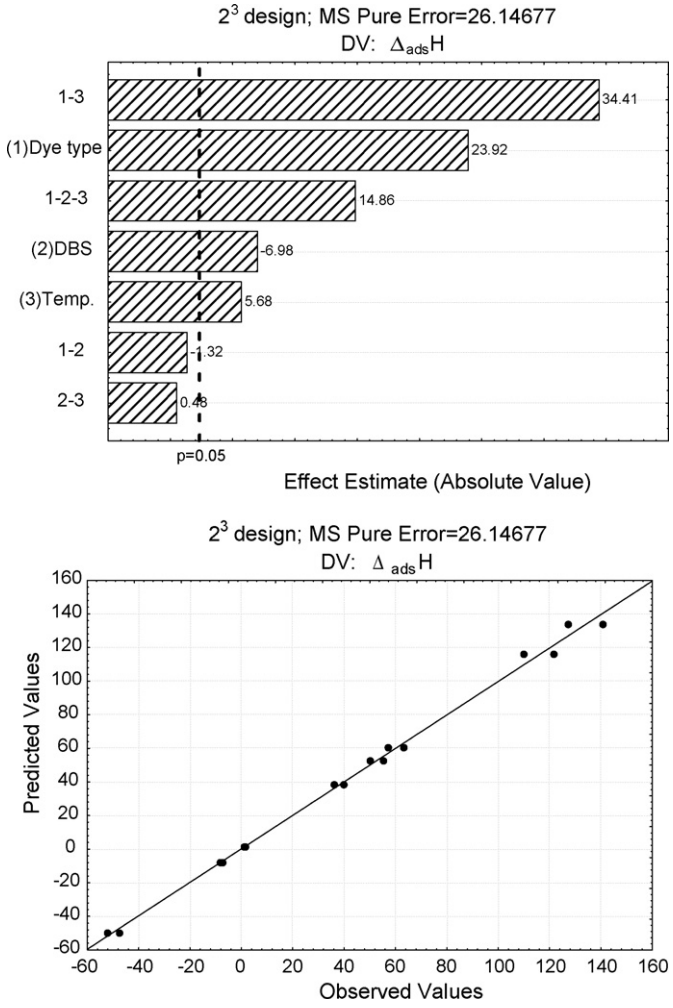

Fig. 10. Pareto chart (upper figure) and the observed vs predicted values confrontation (lower figure) for $\Delta_{ads}H$ in relation to the 2^3 factorial design.

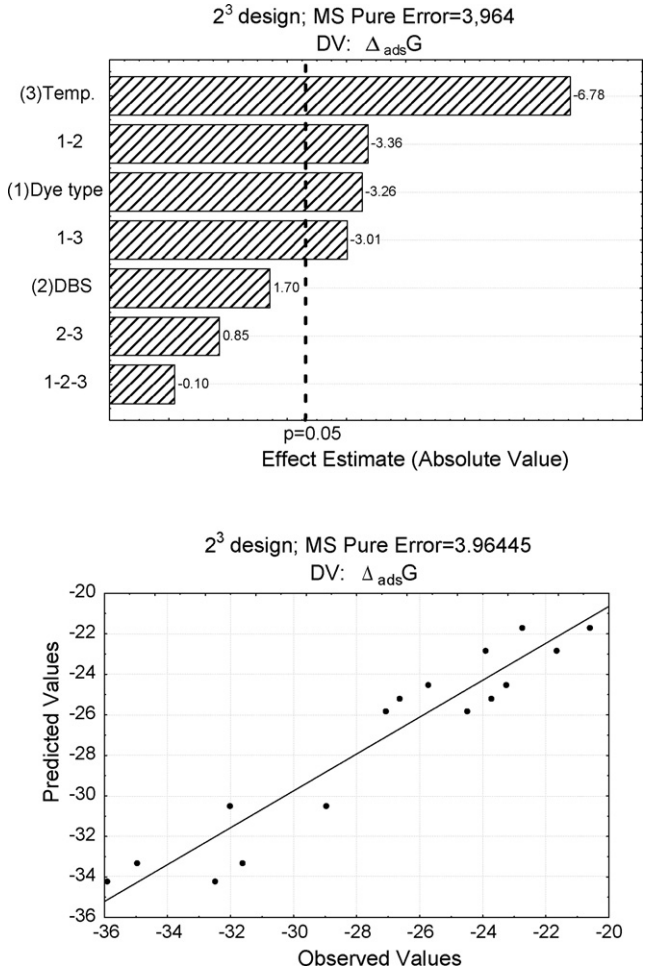

Fig. 11. Pareto chart (upper figure) and the observed vs predicted values confrontation (lower figure) for $\Delta_{ads}G$ in relation to the 2^3 factorial design.

the principal effects of each factor and their interactions on adsorptions at the solid/solution interfaces, as well as those for academic and industrial processes [29,30].

The factorial design results are in Table 4 and the respective principal and interaction effects for the first factorial design study are presented in Table 5. The effects errors were 2.56 kJ mol^{-1}, 1.00 kJ mol^{-1} and 10 J K^{-1} mol^{-1}, for $\Delta_{ads}H$, $\Delta_{ads}G$ and $\Delta_{ads}S$, respectively. If the interaction terms are left out of the models (data not shown) the errors increase significantly.

On average, the use of the red dye causes a significant increase in $\Delta_{ads}H$ and $\Delta_{ads}S$. This is indicated by the effect for dye type of 61.16 kJ mol^{-1} ($\Delta_{ads}H$) and 193 J K ($\Delta_{ads}S$). The presence of DBS decreases the principal effects of both $\Delta_{ads}H$ and $\Delta_{ads}S$. This decrease in the enthalpy has been attributed to the hydrophobic characteristics of the dye/micelle aggregates in solution [31]. On this sight, individually solvated surfactant molecules with the polar groups (SO_3^-) close to the sites occupied by water molecules on surface (step I). At the start of adsorption, the $-SO_3^-$ groups occupy the sites from which the water molecules are replaced and simultaneously driven to the edges of alkyl chains closed to polar heads. The partial surface hydrophobic interactions between the alkyl chains of adsorbed DBS proceed (step II). In general, the adsorbed surfactant layer was built up primarily by the patchwise formation of essentially bilayer aggregates [31,32]. Indeed, the assembly and adsorption of surfactants at the silica/water interface is a complicated process. Besides the electrostatic interaction, which is usually exothermic between the $-SO_3^-$ anions and positively charged Sil-NH_2 surface, some unknown interactions which predominately exhibit endothermic may exist.

The reorientation or restructuring of water around is very unfavorable in terms of entropy, since it disturbs the existing water structure and imposes a new and less ordered structure on the surrounding water molecules. Therefore, the positive values of almost all $\Delta_{ads}S$ in the multivariate analysis suggest the increased randomness at the solid–solution interface during the adsorption of dyes on Sil-NH_2. The principal effect of the presence of DBS is only marginally important in relation to the other multivariate results showed in Table 5.

The variations of the factors did not produce significant effects in $\Delta_{ads}G$ values, which are ruled, mainly, by the temperature changes of the factorial design.

A quantitative reduced model for each thermodynamic parameter of absorbed dyes can be written in terms of the statistically significant effects in Table 5 [29],

$$\Delta_{ads}H = 43.16 + 30.58x_1 - 8.93x_2 + 7.26x_3 + 44.00x_1x_3 + 19.00x_1x_2x_3 \quad (14)$$

$$\Delta_{ads}G = -27.25 - 1.63x_1 - 3.38x_3 - 1.67x_1x_2 - 1.50x_1x_3 \quad (15)$$

$$\Delta_{ads}S = 224 + 97x_1 - 31.7x_2 + 22.7x_3 + 140x_1x_3 + 61.6x_1x_2x_3 \quad (16)$$

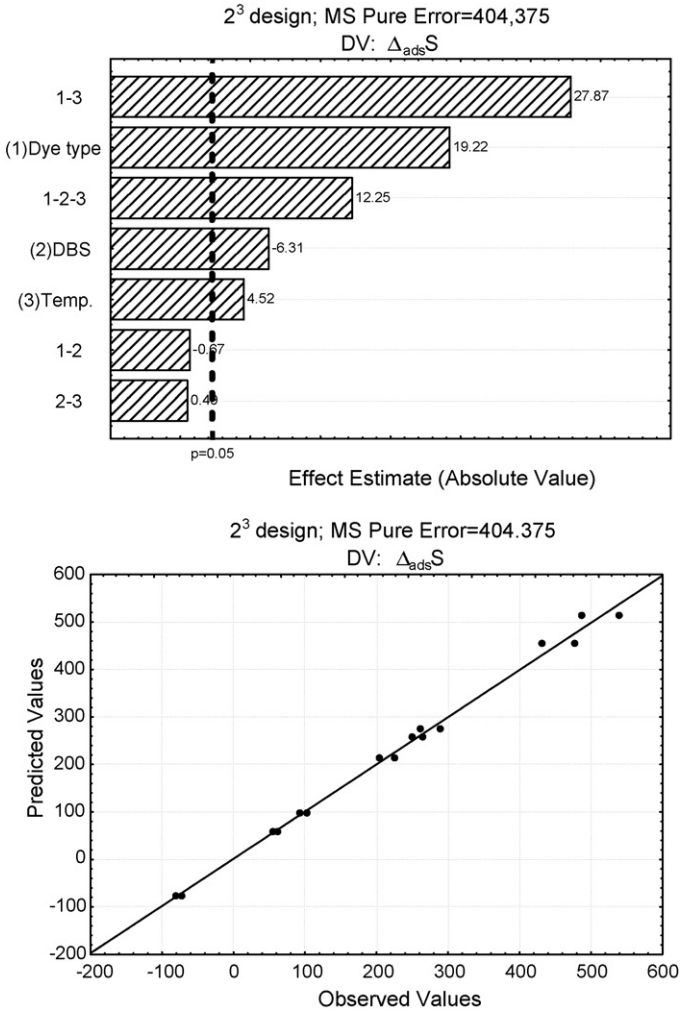

Fig. 12. Pareto chart (upper figure) and the observed vs predicted values confrontation (lower figure) for $\Delta_{ads}S$ in relation to the 2^3 factorial design.

where x_1, x_2 and x_3 are codified (± 1) values of dye type, presence of DBS and temperature, respectively.

The Pareto charts and the predicted vs observed graphical correlations for each thermodynamic parameter are shown in Figs. 10–12. In general, good correlations were observed for $\Delta_{ads}H$ and $\Delta_{ads}S$. In the case of $\Delta_{ads}G$, the lack of fit is due to the absence of the principal effect value of DBS, as well as the three-factor interaction in the model of Eq. (12). This led to a lower statistic degree of correlation in relation to $\Delta_{ads}H$ and $\Delta_{ads}S$.

4. Conclusion

The three-parameter Sips adsorption model was successfully employed to modeled previously published adsorption data of two reactive dyes onto a mesoporous aminopropyl-silica, in the absence and in the presence of the surfactant DBS from 25 to 55 °C. It is observed that the Sips model is a good suitable model to evaluate the adsorptions of the dyes, both in the absence and in the presence of DBS.

The presence of curvatures of the plots ln K vs $1/T$ suggested that the thermodynamic parameters are characterized by non-zero heat capacities terms. This finding is rather unusual for adsorption phenomena at solid/solution interfaces. For the yellow dye, it is observed that the values of $\Delta_{ads}H$ are almost all positive and they decrease in endothermicity, in the absence and in the presence of DBS, from 25 to 55 °C. For the red dye, the opposite situation is observed, i.e., there is an increase in endothermicity in relation to the temperature increase.

The negative values of $\Delta_{ads}G$ indicate that the interactions of the dyes with the Sil-NH_2 silica are spontaneous processes in the absence and in the presence of DBS. The positive adsorption entropy values ($\Delta_{ads}S$) for the interaction of the dyes also suggest that entropy is a driving force of adsorption.

The temperature dependence of the thermodynamics parameters was also evaluated using a new factorial design analysis. The multivariate polynomial modelings indicated that the thermodynamic parameters $\Delta_{ads}H$, $\Delta_{ads}G$ and $\Delta_{ads}S$ are also affected by important interactive effects of the experimental factors and not by the temperature changes alone.

Acknowledgments

The authors thank fellowships to G.S.V. and A.M.G.T. (CNPq, Brazil/PIBIC Program). A.R.C., E.F.S.V., W.L. and C.A. acknowledge fellowships and financial support from CNPq, Brazil and CAPES (Pos-Doctoral program, Process 0014052), Brazil.

References

[1] J.J.M. Órfão, A.I.M. Silva, J.C.V. Pereira, S.A. Barata, I.M. Fonseca, P.C.C. Faria, M.F.R. Pereira, Adsorption of a reactive dye on chemically modified activated carbons—Influence of pH, J. Colloid Interface Sci. 296 (2006) 480–489.
[2] L. Li, S. Wang, Z. Zhu, Geopolymeric adsorbents from fly ash for dye removal from aqueous solution, J. Colloid Interface Sci. 300 (2006) 52–59.
[3] S.G. Wang, R.Z. Wang, X.R. Li, Research and development of consolidated adsorbent for adsorption systems, Renew. Energy 30 (2005) 1425–1441.
[4] A. Dabrowski, P. Podkoscielny, Z. Hubicki, M. Barczak, Adsorption of phenolic compounds by activated carbon—a critical review, Chemosphere 58 (2005) 1049–1070.
[5] B. Kasprzyk-Hordern, Chemistry of alumina, reactions in aqueous solution and its application in water treatment, Adv. Colloid Interface Sci. 110 (2004) 19–48.
[6] E. Pefferkorn, Polyacrylamide at solid/liquid interfaces, J. Colloid Interface Sci. 216 (1999) 197–220.
[7] M.E. Mahmoud, S.S. Haggag, A.H. Hegazi, Synthesis, characterization, and sorption properties of silica gel-immobilized pyrimidine derivative, J. Colloid Interface Sci. 300 (2006) 94–99.
[8] T. Asefa, M.J. Maclachlan, N. Coombs, Periodic mesoporous organosilicas, PMOs: fusion of organic and inorganic chemistry 'inside' the channel walls of hexagonal mesoporous silica, Nature 402 (1999) 867–871.
[9] M. Mifune, K. Kawata, K. Tanaka, Y. Kitamura, I. Tsukamoto, M. Saito, J. Haginaka, Y. Saito, HPLC retention behaviors of poly-aromatic-hydrocarbons on Cu(II)-octabromotetrakis(4-carboxyphenyl)porphine derivatives-immobilized aminopropyl silica gels in polar and non-polar eluents, Chem. Pharm. Bull. 54 (2006) 94–98.
[10] P.G. Zanichelli, R.L. Sernaglia, D.W. Franco, Immobilization of the [Ru-II(edta)NO+] ion on the surface of functionalized silica gel, Langmuir 22 (2006) 203–208.
[11] J.C.C. Chang, S. Cheng, Direct synthesis and catalytic reactivity of highly ordered large-pore methylaminopropyl-functionalized SBA-15 materials, Aust. J. Chem. 233 (2005) 266–275.
[12] T. Seckin, A. Gultek, Postgrafting of Congo red dye onto hyperbranched mesoporous silica with terminal amino groups, J. Appl. Polym. Sci. 90 (2003) 3905–3911.
[13] C. Cooper, R. Burch, Mesoporous materials for water treatment processes, Water Res. 33 (1999) 3689–3694.
[14] A. Andrzejewska, A. Krysztafkiewicz, T. Jesionowski, Treatment of textile dye wastewater using modified sílica, Dyes Pigments 75 (2007) 116–124.
[15] T. Jesionowski, Characterisation of pigments obtained by adsorption of C.I. Basic Blue 9 and C.I. Acid Orange 52 dyes onto silica particles precipitated via the emulsion route, Dyes Pigments 67 (2005) 81–92.
[16] S. Paria, C. Manohar, K.C. Khilar, Kinetics of adsorption of anionic, cationic, and nonionic surfactants, Ind. Eng. Chem. Res. 44 (2005) 3091–3098.
[17] A.R. Cestari, E.F.S. Vieira, G.S. Vieira, L.E. Almeida, Aggregation and adsorption of reactive dyes in the presence of an anionic surfactant on mesoporous aminopropyl silica, J. Colloid Interface Sci. 309 (2007) 402–411.
[18] A.R. Cestari, E.F.S. Vieira, A.A. Pinto, E.C.N. Lopes, Multistep adsorption of anionic dyes on silica/chitosan hybrid – 1. Comparative kinetic data from liquid- and solid-phase models, J. Colloid Interface Sci. 292 (2005) 363–372.
[19] O. Hamdaoui, E. Naffrechoux, Modeling of adsorption isotherms of phenol and chlorophenols onto granular activated carbon. Part II. Models with more than two parameters, J. Hazard. Mater. 147 (2007) 401–411.

[20] A.R. Cestari, E.F.S. Vieira, A.G.P. dos Santos, J.A. Mota, V.P. de Almeida, Adsorption of anionic dyes on chitosan beads. 1. The influence of the chemical structures of dyes and temperature on the adsorption kinetics, J. Colloid Interface Sci. 280 (2004) 380–386.
[21] G. Limousin, J.-P. Gaudet, L. Charlet, S. Szenknect, V. Barthès, M. Krimissa, Sorption isotherms: a review on physical bases, modeling and measurement, Appl. Geochem. 22 (2007) 249–275.
[22] J. Oakes, P. Gratton, Solubilisation of dyes by surfactant micelles. Part 1: molecular interactions of azo dyes with nonionic and anionic surfactants, Color Technol. 119 (2003) 91–99.
[23] A.R. Cestari, E.F.S. Vieira, C.R.S. Mattos, Thermodynamics of the Cu(II) adsorption on thin vanillin-modified chitosan membranes, J. Chem. Thermodyn. 38 (2006) 1092–1099.
[24] A. Ramesh, D.J. Lee, J.W.C. Wong, Thermodynamic parameters for adsorption equilibrium of heavy metals and dyes from wastewater with low-cost adsorbents, J. Colloid Interface Sci. 291 (2005) 588–592.
[25] A.G.S. Prado, J.D. Torres, E.A. Faria, S.C.L. Dias, Comparative adsorption studies of indigo carmine dye on chitin and chitosan, J. Colloid Interface Sci. 277 (2004) 43–47.
[26] G.A. Holdgate, W.H.J. Ward, Measurements of binding thermodynamics in drug discovery, Drug Discov. Today 10 (2005) 1543–1550.
[27] S.K. Parida, S. Dash, S. Patel, B.K. Mishra, Adsorption of organic molecules on silica surface, Adv. Colloid Interface Sci. 121 (2006) 77–110.
[28] P.V. Messina, P.C. Schulz, Adsorption of reactive dyes on titania-silica mesoporous materials, J. Colloid Interface Sci. 299 (2006) 305–320.
[29] R.E. Bruns, I.S. Scarminio, B. de Barros Neto, Statistical Design–Chemometrics, Elsevier, Amsterdam, 2006.
[30] A.R. Cestari, E.F.S. Vieira, A.J.P. Nascimento, C. Airoldi, New factorial designs to evaluate chemisorption of divalent metals on aminated silicas, J. Colloid Interface Sci. 241 (2001) 45–51.
[31] W. Loh, L.A.C. Teixeira, L.-T. Lee, Isothermal calorimetric investigation of the interaction of poly(*N*-isopropylacrylamide) and ionic surfactants, J. Phys. Chem. B 108 (2004) 3196–3201.
[32] X. Geng, F. Xie, H. Zhang, X. Wang, J. Xing, Assembly of sodium dodecyl sulfate at the wool/water interface, Colloids Surf. A 257–258 (2005) 89–98.